Marine Pollution Bulletin 196 (2023) 115622

Contents lists available at ScienceDirect

Marine Pollution Bulletin

journal homepage: www.elsevier.com/locate/marpolbul

Baseline

Assessment of human health risks of toxic elements in coastal area between Al-Khafji and Al-Jubail, Saudi Arabia

Hassan Alzahrani, Abdelbaset S. El-Sorogy *, Saleh Qaysi

Geology and Geophysics Department, College of Science, King Saud University, Saudi Arabia

ARTICLE INFO

Keywords:
Toxic metals
Enrichment factor
Human health risk
Chronic daily intake
Arabia Gulf

ABSTRACT

The present work aims to document the distribution of toxic elements (TEs) and assess the human health risk posed by the TEs in the marine sediment of the Arabian Gulf, Saudi Arabia. The descending order of TE averages (μg/g) was as follows: Ni > Cr > V > Zn > Pb > Cu > As > Co. Based on the enrichment factor values, only minor enrichment for Pb, As, Cr, and Ni was noted. The hazard index (HI) values for the non-carcinogenic risk of the TEs were less than 1.0, and the lifetime cancer risk values for carcinogenic Pb, Cr, and As ranged between 2.96×10^{-8} and 5.44×10^{-5}, indicating no significant health hazards for the inhabitants of the study area.

Toxic elements (TEs) enter marine environments through anthropogenic and geogenic sources. The principal anthropogenic sources for TEs include mining and smelting operations; industries (textile, pharmaceuticals, petrochemicals, ceramics, oil mills, sugar industries, and fertilizer factories); domestic effluents; sewage sludge; coal burning in power plants; nuclear power stations; and agricultural applications of chemicals containing metals and metal-containing compounds (Goyer, 1993; Rehman et al., 2008; Häder et al., 2021). Natural sources of TEs include metal-bearing igneous, sedimentary and metamorphic rocks and soil formation (Al-Kahtany et al., 2015; Alharbi and El-Sorogy, 2019). Sediment or dust ingestion, skin contact, and inhalation are the three pathways by which the TEs enter the human body (Naveedullah et al., 2014). Excessive TE consumption in humans can result in neurological; cardiovascular; and chronic kidney illness; tumors and cancer (Song and Li, 2014; Pan et al., 2018a; Alfaifi et al., 2021). Children are more vulnerable to TEs due to additional exposure pathways such as nursing, placental exposure, early-life hand-to-mouth activities, adolescent risk-taking, larger comparative uptakes, and lower toxin elimination rates (Dissanayake and Chandrajith, 2009; Ma et al., 2016; Rahman et al., 2021).

The accumulation of TEs in human bodies may cause harmful complications. For example, Pb accumulation results in lead poisoning, giving rise to chronic health problems such as blood disorders, brain and nerve disorders, cardiovascular problems, mineralizing of bones and teeth, structural damage and changes in the excretory function of kidneys, digestive problems, and hypertension (Yuan et al., 2014; Abadin et al., 2007). Population exposure to high levels of As causes a myriad of serious health problems such as lung diseases, cardiovascular diseases, oxidative stresses, diabetes, various types of cancers, a decrease in white and red blood cells production, gastrointestinal irritation, hyperkeratosis and pigmentation (Järup, 2003; Huy et al., 2014). Moreover, Cd-toxicity causes several severe ailments including damage to the lungs and respiratory irritation, stomach irritation, kidney damage, soft or brittle bones, defects in the endocrine system and cancer (Nishijo et al., 2017; Mao et al., 2019).

As the Arabian Gulf is a shallow basin, pollution from human activities such as industrial and sewage effluents may significantly alter and damage the marine ecosystem and environment of the Arabian Gulf (Al-Kahtany et al., 2023; Alharbi et al., 2022; Al-Hashim et al., 2022; Al-Kahtany and El-Sorogy, 2022, 2023). Al-Khafji and Al-Jubail cities are located in the northeast of Saudi Arabia, along the Arabian Gulf. El-Sorogy and Youssef (2015) studied the accumulation of TEs in several mollusk shells in the Al-Jubail coastal area and concluded that petrochemical industries, antifouling chemicals, oil leakage, desalination plants, and sewage effluents were the primary anthropogenic sources of TEs in mollusk shells. Alharbi et al. (2017) documented anthropogenic contributions for TEs in sediments of the Al-Khafji coastal area, and attributed their higher levels to desalination plants, landfilling, industrial sewage, and oil pollutants.

Many studies dealing with TE evaluation utilizing various pollution indices have been conducted on the coastal sediment along the east and west coastlines of the Arabian Gulf over the last three decades (e.g. geoaccumulation index, enrichment factor, contamination factor, pollution load index, degree of contamination, and modified degree of

* Corresponding author at: P.O Box: 2455, Riyadh 11451, Saudi Arabia.
E-mail address: asmohamed@ksu.edu.sa (A.S. El-Sorogy).

https://doi.org/10.1016/j.marpolbul.2023.115622
Received 23 June 2023; Received in revised form 27 September 2023; Accepted 2 October 2023

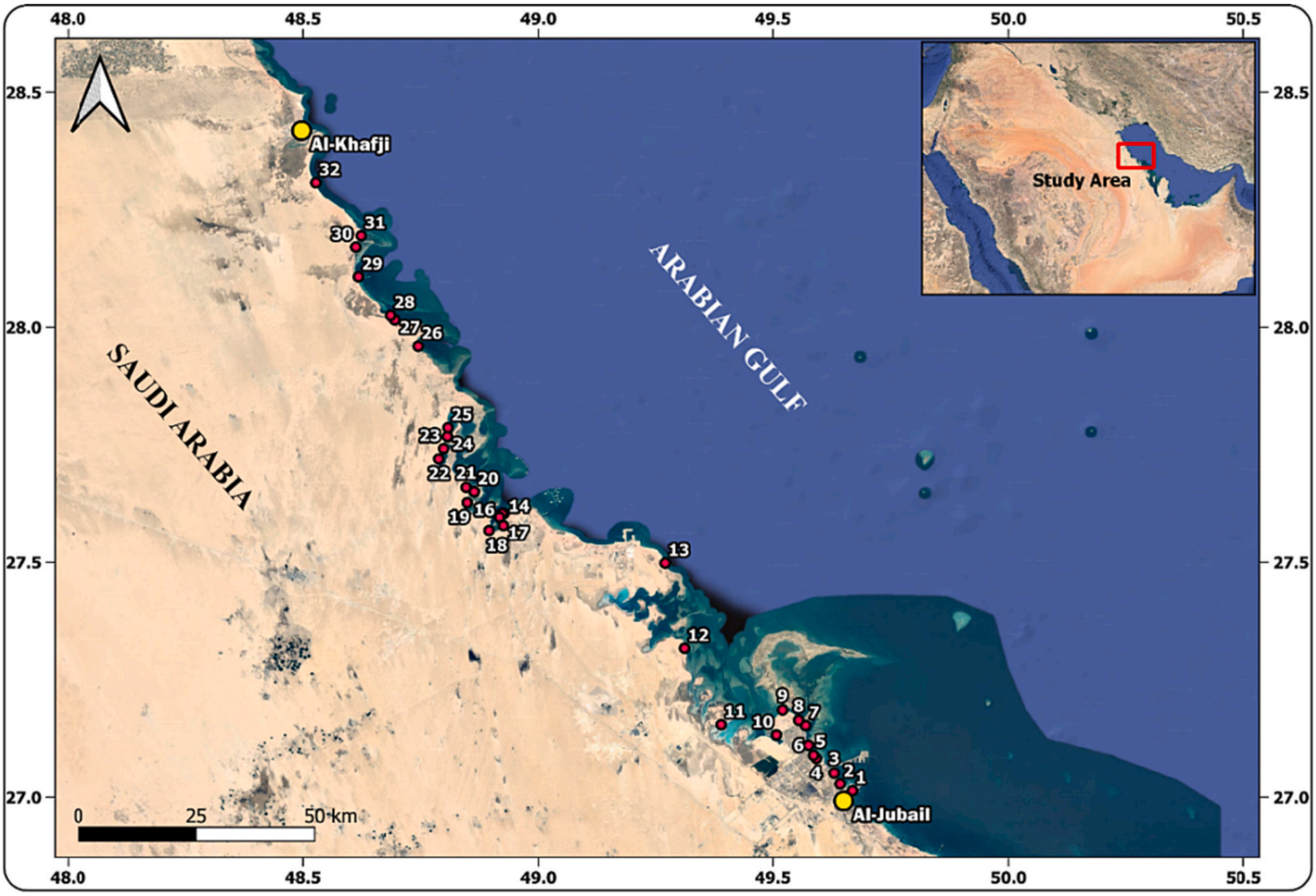

Fig. 1. Location map of the study area along the Arabian Gulf and the sampling sites.

Table 1
The average values of TEs (dw, μg/g) in the study area and the comparison with those reported in the earth's crust and international backgrounds.

Location	As	V	Cr	Zn	Cu	Pb	Ni	Co	References
Arabian Gulf, Saudi Arabia	2.38	7.35	8.68	6.18	2.44	2.57	11.76	1.25	Present study
Ras Abu Ali Island, Saudi Arabia	2.47	6.67	7.86	6.89	4.14	3.50	13.00	1.43	Al-Kahtany and El-Sorogy (2023)
Aqeer coastline, Arabian Gulf	15	NA	3.67	7.62	11.27	3.88	0.57	NA	Al-Hashim et al. (2021)
Red Sea-Gulf of Aqaba, Saudi Arabia	133	NA	39	24	30	6.60	14	4.5	El-Sorogy et al. (2020a)
Jazan area, Red Sea, Saudi Arabia	NA	NA	32.9	28.5	31.6	2.3	20	4.13	Kahal et al. (2020)
Al-Khobar, Arabian Gulf, Saudi Arabia	1.61	268	51.0	52.7	183	5.4	75	4.75	Alharbi and El-Sorogy (2017)
Mediterranean Sea, Egypt	298	375	0.18	183	24.57	385	481	69.8	El-Sorogy et al. (2016)
Background shale	13	130	90	95	45	20	68	19	Turekian and Wedepohl (1961)
Background Earth's crust	1.7	97	83	67	47	16	58	18	Yaroshevsky (2006)

NA: not available.

contamination). Most of these studies have not taken the human health assessment into consideration. Therefore, the objectives of the present work are to; (i) document the distribution of V, As, Co, Ni, Zn, Cr, Pb, and Cu in the marine sediment in the coastal area between Al-Khafji and Al-Jubail cities along the Arabian Gulf; (ii) assess the degree of enrichment and ecological risk caused by these TEs; and (iii) determine the cumulative carcinogenic and non-carcinogenic risks of TEs using the chronic daily intake (CDI), hazard index (HI), and total lifetime cancer risk (LCR) via ingestion and dermal pathways in both adults and children.

The study area is located between Al-Jubail and Al-Khafji along the Arabian Gulf coast, Saudi Arabia, between N27° 00′ 84″ – N28° 18′ 26″ and E49° 40′ 00″ – E48° 31′ 37″ (Fig. 1). The coastline in the study area is sandy and has rocky shores with biogenic concentrations of barnacles, worm tubes and gastropods. The rocks of the rocky shores and their inhabited mollusks have been bio-eroded by endolithic bivalves, polychaete annelids, clionid sponges, durophagous drillers, vermetid gastropods, and acorn barnacles. The same rocky shore dwellers can be identified from many coastal areas along the Red Sea and the Arabian Gulf coasts (El-Sorogy, 2015; El-Sorogy et al., 2018, El-Sorogy et al., 2020a, El-Sorogy et al., 2021; Demircan et al., 2021). Generally, the biogenic quotient along the coastline drifts from offshore during storms and tides, while the terrestrial part comes from the hinterland Quaternary sediments (Alzahrani et al., 2023). In the current study, surface sediment samples were collected in January 2022 from the coastal zone of thirty-two sites (Fig. 1). The sediments were stored in plastic bags and placed in an ice box before they were transported to the laboratory where they were dried and sieved.

The sediments were analysed for the presence of Ni, Cu, Cr, As, Zn, V, Co, and Pb, using Inductively Coupled Plasma - Atomic Emission

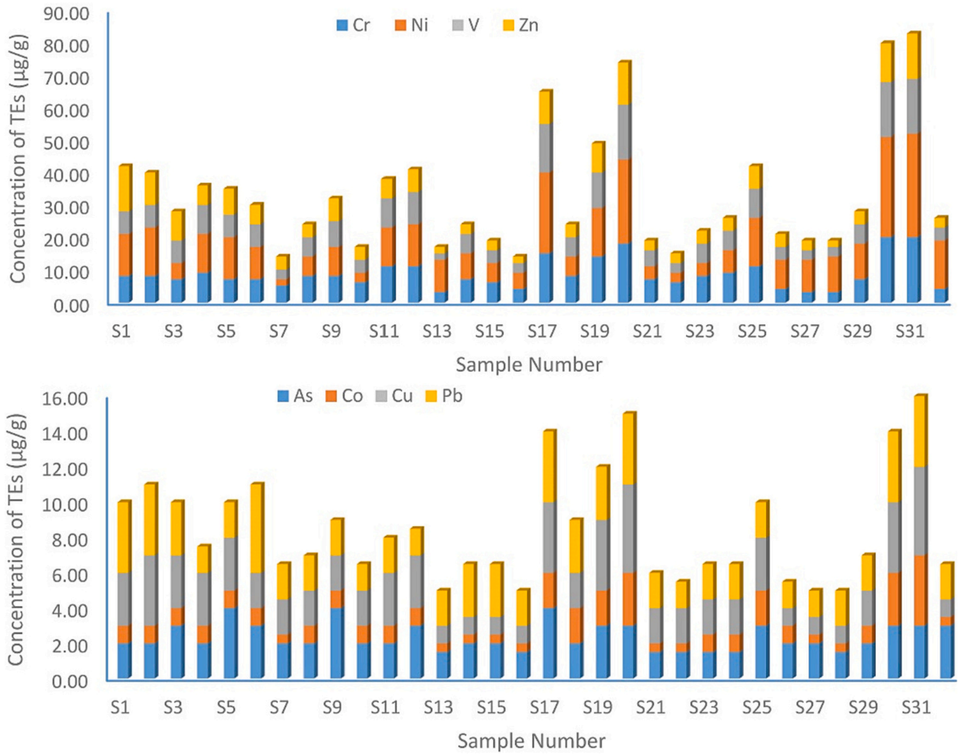

Fig. 2. Mean concentration (based on dry weight, dw) of toxic elements in the sediment samples from the study area.

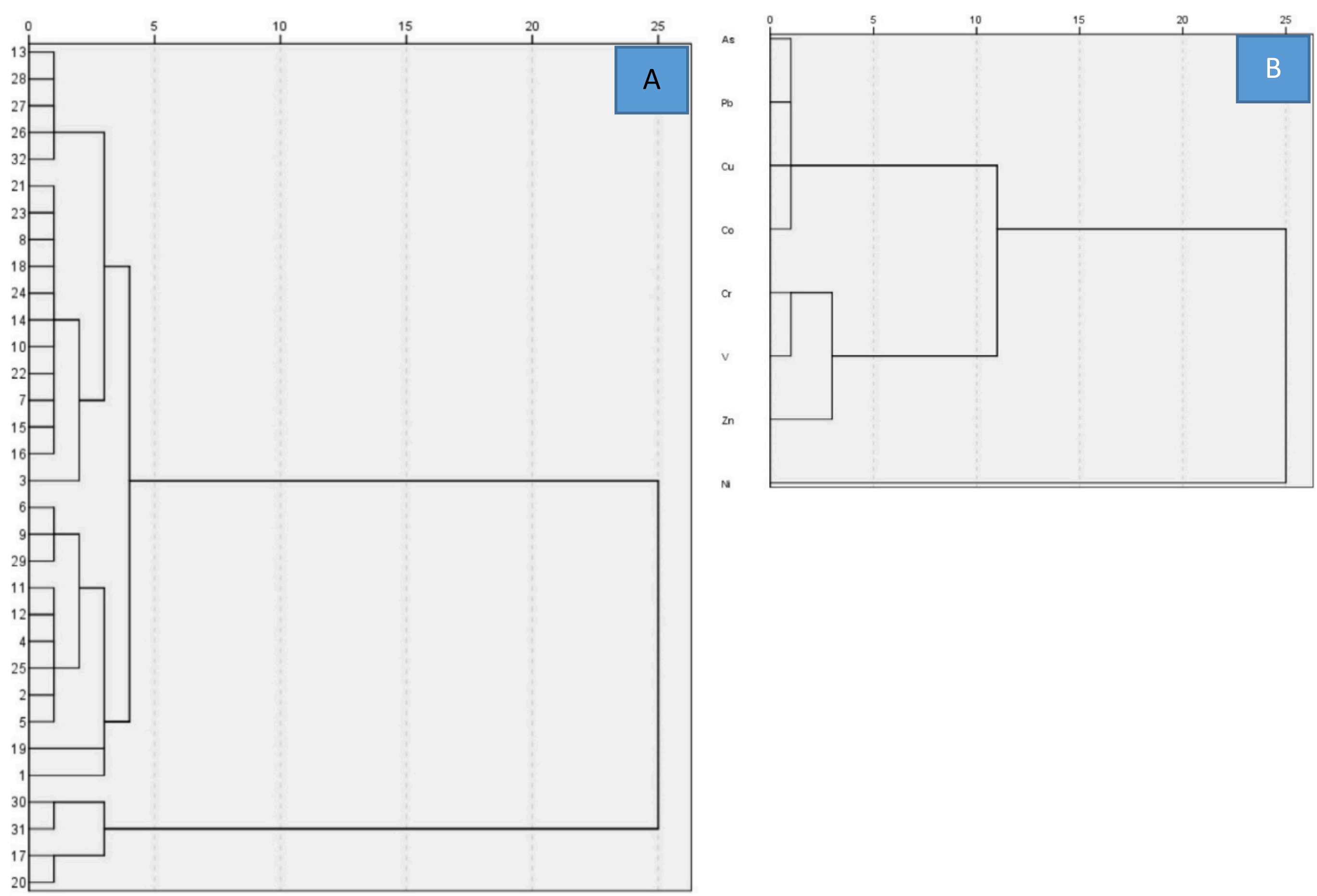

Fig. 3. Q-mode HCA (A) of the sediment samples and R-mode HCA (B) of the TEs in the study area.

Table 2
Minimum, maximum and average values of EF and Eri.

	EF			Er^i		
	Min.	Max.	Avg.	Min.	Max.	Aver.
Pb	0.31	4.43	1.64	0.38	1.25	0.64
As	0.51	4.64	1.87	1.15	3.08	1.83
Zn	0.18	2.79	0.78	0.02	0.15	0.07
Ni	0.16	7.54	2.12	0.18	2.82	1.03
Cu	0.19	2.62	0.70	0.11	0.56	0.27
Co	0.14	3.11	0.83	0.01	0.09	0.03
Cr	0.29	4.59	1.27	0.07	0.44	0.19
V	0.12	2.50	0.72	0.03	0.26	0.11

Spectroscopy (ICP – AES) in ALS Geochemistry Laboratory, Jeddah branch, Saudi Arabia. A part of the prepared sample (0.50 g) was digested with aqua regia (a mixture of one mole of nitric acid and three moles of hydrochloric acid) for 45 min in a graphite heating block. After the mixture had cooled, the resulting solution was diluted to 12.5 mL with deionized water, mixed and analysed. The analytical results were corrected for inter–element spectral interferences. Validation of the ICP–AES technique was performed regarding linearity, limit of detection (LOD), and limit of quantification (LOQ) (Papadoyannis and Samanidou, 2004; Christodoulou and Samanidou, 2007). The calibration procedure was performed by the preparation of a stock standard solution of all investigated elements with concentrations of 1000 mg/kg. The single–element solutions of each of the investigated elements with concentrations of 1, 5, and 10 mg/kg, respectively, were prepared from stock solutions by dilution with tridistilled water. The ALS Geochemistry Laboratory has established a sound quality control/quality assurance experience and protocol over many similar studies throughout the years (Alzahrani et al., 2023). The coordinates of the samples and the concentrations of the TEs (μg/g, dry weight) are presented in Supplementary Table 1. Hierarchical clustering analysis (HCA) and Pearson's correlation coefficients were used as multivariate statistical tools to identify the possible sources of the TEs.

The enrichment factor (EF) and potential ecological risk (RI) values were used to evaluate sediment contamination with particular TEs and determined whether the TE content in sediment was affected by human activities or natural factors (Kowalska et al., 2018; Huang et al., 2022). Supplementary Table 2 shows the classification of these indices. The EF was calculated to assess the proportion of the metals in excess with respect to the lithological background, according to the following formula:

$$EF = (M/X)_{sample} \div (M/X)_{background}$$

where M is the analysed metal and X is the level of a normalizer element. Fe was chosen as the normalizing element due to its high content and relatively stable chemical properties and not easily affected by the external environment (Bryanin and Sorokina, 2019).

RI was used to assess the degree of the ecological risk caused by TEs in coastal sediments (Hakanson, 1980). It was calculated using the following equation:

$$Er^i = Tr^i \times Cf^i$$

$$RI = \sum (Tr \times CF)$$

where Eri is the potential ecological risk factor of an individual element, Tr is the toxicity response coefficient of an individual metal (Zn = Co = 1, Cr = 2, Cu = Pb = 5, Ni = 6, As = 10) (Hakanson, 1980); and CF is the contamination factor (Supplementary Table 2). The health risks via ingestion and dermal contact pathways in both adults and children were calculated according to the Environmental Protection Agency of the United States (US EPA). The chronic daily intake (CDI) for the two pathways (mg/kg/ day) was estimated according to the following equations (Luo et al., 2012; Mondal et al., 2021; Škrbić et al., 2022):

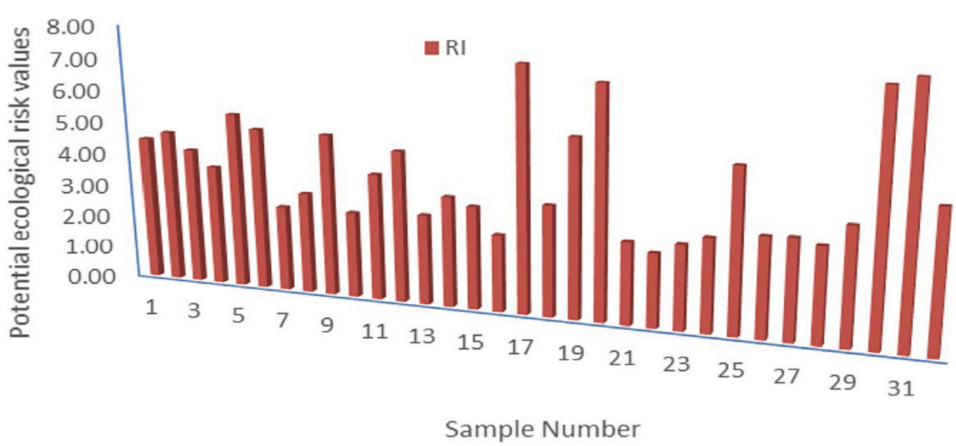

Fig. 4. The calculated RI values for the sediment samples in the study area.

Table 3
Pearson's correlation coefficients of the investigated TEs.

	As	Co	Cr	Cu	Ni	Pb	V	Zn
As	1							
Co	0.470**	1						
Cr	0.495**	**0.908****	1					
Cu	**0.520****	**0.801****	**0.879****	1				
Ni	**0.556****	**0.819****	**0.817****	**0.731****	1			
Pb	0.363*	**0.548****	**0.550****	**0.551****	**0.571****	1		
V	**0.612****	**0.888****	**0.972****	**0.883****	**0.870****	**0.585****	1	
Zn	**0.580****	**0.753****	**0.790****	**0.897****	**0.757****	**0.680****	**0.832****	1

** Correlation is significant at the 0.01 level (2-tailed).
* Correlation is significant at the 0.05 level (2-tailed).

Table 4
The CDI (mg/kg/day), HQ and HI for non-carcinogenic risk in adults and children.

HEs	Adults				
	CDI $_{Ing.}$	CDI $_{Dermal}$	HQ $_{Ing.}$	HQ $_{Demal}$	HI
As	3.232×10^{-6}	1.290×10^{-8}	1.077×10^{-2}	4.299×10^{-5}	1.082×10^{-2}
Cr	1.164×10^{-5}	4.646×10^{-8}	3.881×10^{-3}	1.549×10^{-5}	3.897×10^{-3}
Pb	3.467×10^{-6}	1.384×10^{-8}	9.907×10^{-4}	3.953×10^{-6}	9.947×10^{-4}
V	9.889×10^{-6}	3.946×10^{-8}	1.099×10^{-3}	4.384×10^{-6}	1.103×10^{-3}
Cu	3.296×10^{-6}	1.315×10^{-8}	8.885×10^{-5}	3.545×10^{-7}	8.920×10^{-5}
Ni	1.567×10^{-5}	8.199×10^{-8}	7.556×10^{-4}	4.099×10^{-6}	7.597×10^{-4}
Zn	8.305×10^{-6}	1.640×10^{-8}	2.768×10^{-5}	5.466×10^{-8}	2.773×10^{-5}
Co	1.627×10^{-6}	2.733×10^{-9}	8.134×10^{-5}	1.366×10^{-7}	8.147×10^{-5}

HEs	Children				
	CDI $_{Ing.}$	CDI $_{Dermal}$	HQ $_{Ing.}$	HQ $_{Demal}$	Hi
As	3.016×10^{-5}	6.018×10^{-8}	1.006×10^{-1}	2.006×10^{-4}	1.008×10^{-1}
Cr	1.087×10^{-4}	2.168×10^{-7}	3.623×10^{-2}	7.227×10^{-5}	3.630×10^{-2}
Pb	3.236×10^{-5}	6.456×10^{-8}	9.247×10^{-3}	1.845×10^{-5}	9.265×10^{-3}
V	9.229×10^{-5}	1.841×10^{-7}	1.025×10^{-2}	2.046×10^{-5}	1.028×10^{-2}
Cu	3.076×10^{-5}	6.138×10^{-8}	8.292×10^{-4}	6.875×10^{-7}	8.299×10^{-4}
Ni	1.462×10^{-4}	3.826×10^{-7}	7.312×10^{-3}	1.913×10^{-5}	7.331×10^{-3}
Zn	7.751×10^{-5}	7.652×10^{-8}	2.584×10^{-4}	2.551×10^{-7}	2.586×10^{-4}
Co	1.518×10^{-5}	1.275×10^{-8}	7.591×10^{-4}	6.377×10^{-7}	7.598×10^{-4}

$$CDI_{ingest.} = (Csediment \times IngR \times EF \times ED/BW \times AT) \times CF$$

$$CDI_{dermal} = (Csediment \times SA \times AFsediment \times ABS \times EF \times ED/BW \times AT) \times CF$$

The exposure factors used in the estimation of the CDI are presented in Table 1. Cr, Pb and As were selected to estimate the carcinogenic health risks (IARC, 2012), whilst; V, As, Co, Ni, Zn, Cr, Pb, and Cu were also estimated for their non-carcinogenic risk. The hazard index (HI) was estimated by summing up all the hazard quotients (HQs), presenting the total risk of being non-carcinogenic for a single element as follows (Chonokhuu et al., 2019):

$$HI = \Sigma HQ = HQ_{ing} + HQ_{dermal}$$

$$HQ = CDI/RfD,$$

where RfD is the reference dose for each TE (Supplementary Table 3). HI values less than one indicate no significant risk of non-carcinogenic effects, and HI values exceeding one indicate the probability that non-carcinogenic risk effects may occur, and this probability increases with increasing HI (USEPA, 2001; IRIS, 2020). The lifetime cancer risk (LCR) was determined using the following equations:

$$\text{Cancer risk (CR)} = CDI \times CSF$$

$$LCR = \Sigma\text{Cancer Risk} = \text{Cancer risk}_{ing} + \text{Cancer risk}_{dermal}$$

where CSF is the carcinogenic slope factor values (mg/kg.day) for Cr, Pb and As (0.5, 0.0085 and 1.5, respectively) IRIS, 2020. LCR values lower than 1×10^{-6} indicate no significant health hazards, between 1×10^{-6} and 1×10^{-4} indicate acceptable carcinogenic risk, and higher than 1×10^{-4} means the risk is unacceptable (USEPA, 2002; IARC, 2012).

The average values of the TEs in the study area and their comparison with those reported in the earth's crust and international backgrounds are presented in Table 1. The descending order of the TE averages (μg/g) was as follows: Ni (11.76) > Cr (8.68) > V (7.35) > Zn (6.18) > Pb (2.57) > Cu (2.44) > As (2.38) > Co (1.25). The average values of the TEs were less than those reported in Table 1 from the Mediterranean Sea, earth crust and shale backgrounds (Yaroshevsky, 2006; Turekian and Wedepohl, 1961; El-Sorogy et al., 2016). Also, our average values were less than those reported from Al-Khobar, Arabian Gulf, Saudi Arabia (Alharbi and El-Sorogy, 2017), except for the average value of As. Moreover, our average values for As, Zn, Cu, and Pb were less than those from the Aqeer coastline, Arabian Gulf (Al-Hashim et al., 2021), and Red Sea-Gulf of Aqaba, Saudi Arabia (El-Sorogy et al., 2020b). Fig. 2 documents the distribution of the TEs all over the study area. Q-mode HCA identified the collected samples into the following three clusters (Fig. 3A): "S3, S7, S8, S10, S13-S16, S18, S21-S24, S26-S28, S32"; "S1, S2, S4-S6, S9, S11, S12, S19, S25, S29"; and "S17, S20, S30, S31." Samples of the first cluster include the lowest values of all investigated TEs. The second cluster accounted for the highest Pb, while the third cluster included the highest concentration of all TEs, except Pb.

Results of the EF indicated no enrichment for Zn, Cu, Co, and V (averages 0.78, 0.70, 0.83, and 0.72, respectively). The average values of EF for Pb, As, Cr, and Ni were 1.64, 1.87, 1.27, and 2.12, respectively (Table 2), implying minor enrichment in these TEs. Some individual samples, such as S17 showed moderately severe enrichment for Ni (EF = 7.54) and moderate enrichment for Pb (EF = 4.43). The EF values of the sampling points of As (94.10 %), Ni (76.50 %), Pb (76.50 %), Cr (41.20 %), V (17.60 %), Co (17.60.5 %), and Zn (14.7 %) were greater than one, implying that these TEs were more or less interfered by human-caused factors (Huang et al., 2023). Particularly, 5.9 % of As and Ni samples had relatively severe enrichment, which was primarily localized in the middle part of the study area (S17-S20), showing that As and Ni were significantly affected by human activities in this area.

RI values ranged from 2.24 to 7.63, with an average of 4.16, which indicated a no-to-low risk for the investigated TEs in the studied coastal sediments (Supplementary Table 1). Fig. 4 indicates that the higher values of RI were recorded in S17, S20, S30, and S31 (samples of the third cluster, which accounted most of the highest TEs concentrations in the study area). Pearson's correlation coefficients (Table 3) indicated significant positive correlations among many elemental pairs, such as the correlation between each Zn, Co, and Ni, and the remaining TEs, implying similar behavior and source for these TEs (Kahal et al., 2020). R-mode HCA clustered the investigated TEs into two (Fig. 3B): Zn, Cr, Pb, V, As, Co, and Cu in one cluster; and Ni in the other. The TEs of the first cluster showed average EF values less than 2, indicating natural sources for these TEs (Škrbić et al., 2017, 2018b; Kahal et al., 2018). The average value of the EF for Ni was slightly greater than 2, implying some anthropogenic contributions (Škrbić et al., 2017, Škrbić and Marinković, 2019; Alshehri et al., 2021).

Table 4 presents the results of the CDI, HQ, and HI values for non-carcinogenic risk of TEs from ingestion and dermal contact pathways in adults and children. The CDI values of the non-carcinogenic risk for adults and children were greater through the ingestion pathway than through the dermal pathway. The maximum CDI values (mg/kg. day) through the ingestion and dermal pathways for adults were 1.567×10^{-5} and 8.199×10^{-8}, respectively, and the same for children were 1.462×10^{-4} and 3.826×10^{-7}, respectively. However, the CDI values from the ingestion pathways in children for all TEs were approximately nine times than that in adults.

The HI values varied from 2.773×10^{-5} (Zn) to 1.082×10^{-2} (As) for

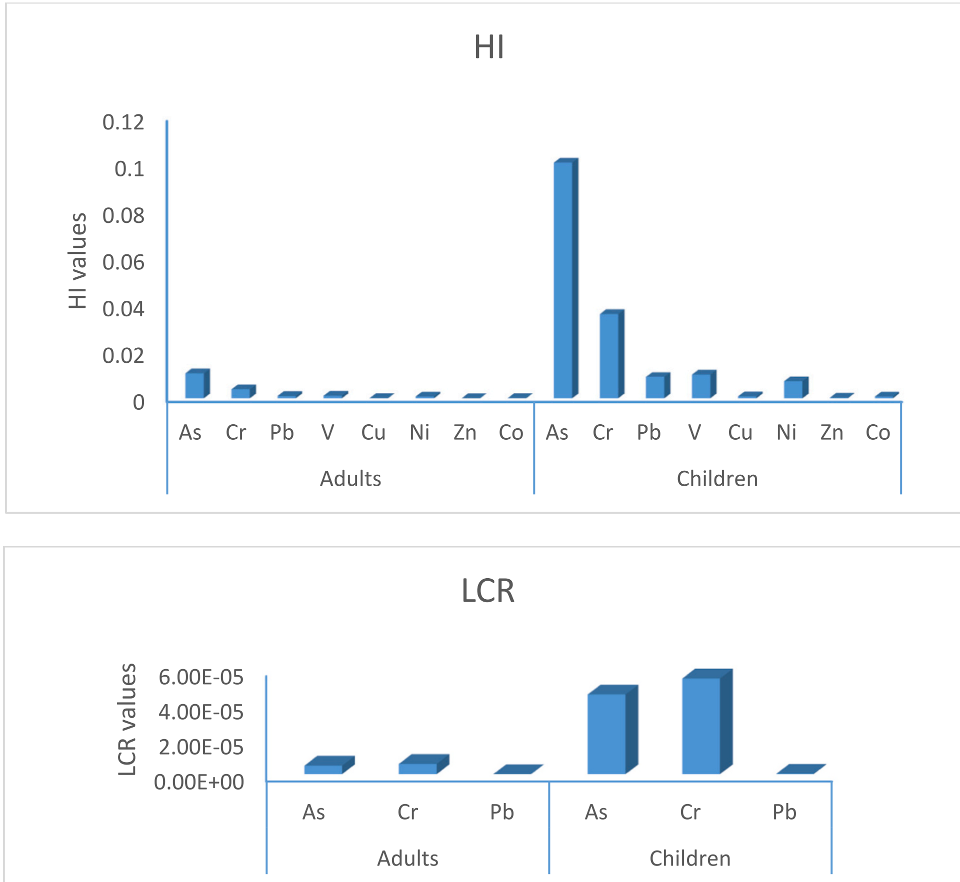

Fig. 5. The HI for non-carcinogenic risk and LCR for or Cr, Pb, and As in adults and children.

Table 5
Carcinogenic risks for Cr, Pb, and As, and LCR for adults and children via ingestion and dermal contact.

HEs	Adults			Children		
	$CR_{Ing.}$	CR_{Dermal}	LCR	$CR_{Ing.}$	CR_{Dermal}	LCR
As	4.848×10^{-6}	1.934×10^{-8}	4.86737×10^{-6}	4.525×10^{-5}	9.027×10^{-8}	4.53386×10^{-5}
Cr	5.822×10^{-6}	2.323×10^{-8}	5.84515×10^{-6}	5.434×10^{-5}	1.084×10^{-7}	5.44463×10^{-5}
Pb	2.947×10^{-8}	1.176×10^{-10}	2.95911×10^{-8}	2.751×10^{-7}	5.488×10^{-10}	2.75635×10^{-7}

adults and from 2.586×10^{-4} (Zn) to 1.008×10^{-1} (As) for children (Fig. 5). The cumulative HI value for the TEs was 9 to 9.5 times higher in children than that in adults regarding the non-carcinogenic risk. Higher HI values in children may be attributed to children's higher sensitivity to exposure and absorption of TEs during their play activities in coastal sediments (Bello et al., 2019). For both adults and children, the HI values exhibited the following descending order: As > Cr > V > Pb > Ni > Cu > Co > Zn.

The contribution of HQ from ingestion to HI for adults and children accounted for 99.60 % and 99.80 % of the total risk, respectively, while the contribution of HQ from dermal accounted for the remaining very small percent. US EPA considered an overall HI value of 1.0 as an acceptable threshold below which no observable clinical effect was reported in experimental animals. HI values for the TEs in the study area were less than 1.0, suggesting no significant non-carcinogenic risk to the people inhabiting the study area (Tian et al., 2020). However, the HI value for As was greater than 0.1 for children, indicating the need to protect them from As ingestion.

The carcinogenic risks for Cr, Pb, and As were estimated in the studied samples. The maximum carcinogenic risk values for adults were 5.822×10^{-6} and 2.323×10^{-8}, and the same for children were 5.434×10^{-5} and 1.084×10^{-7}, through the ingestion and dermal pathways, respectively (Table 5, Fig. 5). The carcinogenic risks in children were approximately nine times higher for ingestion pathway and five times higher for each of dermal and inhalation pathways than those in adults. The contribution of CR_{ing}, and CR_{dermal} to LCR values in adults and children were 99.60 % and 99.80 % and 0.40 % and 0.20 %, respectively. The LCR values of HEs for both adults and children exhibited the following descending order: Cr > As > Pb (Fig. 4). In adults, LCR values ranged from 2.959×10^{-8} (Pb) to 5.845×10^{-6} (Cr); for children, they ranged from 2.756×10^{-7} (Pb) to 5.445×10^{-5} (Cr). US EPA considered an acceptable cancer risk of 1×10^{-6} to 1×10^{-4} for regulatory purposes. However, the LCR values were less than the US EPA's acceptable values, indicating no significant health hazards from the carcinogenic Pb, Cr, and As in the study area (Mondal et al., 2021), despite the risk in children being higher than that in adults, which may be due to the children's finger sucking behavior (Zhao et al., 2013; Pan et al., 2018b; Škrbić et al., 2018a).

This study highlighted the health risk assessment of Ni, Cu, Cr, As, Zn, V, Co, and Pb in the coastal area between Al-Khafji and Al-Jubail, Saudi Arabia. The CDI values of the non-carcinogenic for adults and children risk took the order of ingestion pathway > dermal pathway. EF and RI values indicated no to minor enrichment and low risk of TEs, which originated mostly from natural sources with minor anthropogenic contributions. Determination of HI for non-carcinogenic risk of TEs and the carcinogenic risks for Cr, Pb, and As indicated no significant health hazards, and the studied coastline between Al-Jubal and Al-Khafji cities is safe for vacationers, tourism, and marine activities. The present study could serve as a baseline for TE risks associated with the study area to monitor improvements or further degradation over time.

CRediT authorship contribution statement

Hassan Alzahrani: collecting samples, preparing samples, interpreting chemical analysis, writing manuscript; Abdelbaset El-Sorogy: collecting samples, preparing samples, interpreting chemical analysis, writing manuscript, submitting manuscript; Saleh Qaysi: preparing samples, interpreting chemical analysis, writing manuscript.

Declaration of competing interest

The authors declare that they have no known competing financial interests or personal relationships that could have appeared to influence the work reported in this paper.

Data availability

Data will be made available on request.

Acknowledgements

The authors extend their appreciation to Researchers Supporting Project number RSP2023R425, King Saud University, Riyadh, Saudi Arabia. Moreover, the authors thank the anonymous reviewers for their valuable suggestions and constructive comments, and the editor to improve the quality of the manuscript.

Appendix A. Supplementary data

Supplementary data to this article can be found online at https://doi.org/10.1016/j.marpolbul.2023.115622.

References

Abadin, H., Ashizawa, A., Stevens, Y., Llados, F., Diamond, G., Sage, G., Quinones, A., Bosch, S., Swarts, S., 2007. Toxicological Profile for Lead, Atlanta (GA): Agency for Toxic Substances and Disease Registry (US). Lewis Publishers, Boca Raton.

Alfaifi, H.J., El-Sorogy, A.S., Qaysi, S., Kahal, A., Almadani, S., Alshehri, F., Zaidi, F.K., 2021. Evaluation of heavy metal contamination and groundwater quality along the Red Sea coast, southern Saudi Arabia. Mar. Pollut. Bull. 163, 111975. https://doi.org/10.1016/j.marpolbul.2021.111975.

Alharbi, T., El-Sorogy, A., 2019. Assessment of seawater pollution of the Al-Khafji coastal area, Arabian gulf, Saudi Arabia. Environ. Monit. Assess. 191, 383. https://doi.org/10.1007/s10661-019-7505-1.

Alharbi, T., El-Sorogy, A.S., 2017. Assessment of metal contamination in coastal sediments of Al-Khobar area, Arabian gulf, Saudi Arabia. J. Afr. Earth Sci. 129, 458–468. https://doi.org/10.1016/j.jafrearsci.2017.02.007.

Alharbi, T., Alfaifi, H., Almadani, S.A., El-Sorogy, A., 2017. Spatial distribution and metal contamination in the coastal sediments of Al-Khafji area, Arabian gulf, Saudi Arabia. Environ. Monit. Assess. 189, 634. https://doi.org/10.1007/s10661-017-6352-1.

Alharbi, T., Al-Kahtany, Kh., Nour, H.E., Giacobbe, S., El-Sorogy, A.S., 2022. Contamination and health risk assessment of arsenic and chromium in coastal sediments of Al-Khobar area, Arabian gulf, Saudi Arabia. Mar. Pollut. Bull. 185, 114255. https://doi.org/10.1016/j.marpolbul.2022.114255.

Al-Hashim, M.H., El-Sorogy, A.S., Al Qaisi, S., Alharbi, T., 2021. Contamination and ecological risk of heavy metals in Al-Uqair coastal sediments, Saudi Arabia. Mar. Pollut. Bull. 171, 112748. https://doi.org/10.1016/j.marpolbul.2021.112748.

Al-Hashim, M.H., El-Sorogy, A.S., Alshehri, F., Qaisi, S., 2022. Environmental assessment of surface seawater in Al-Uqair coastline, Eastern Saudi Arabia. Water 2022 (14), 3423. https://doi.org/10.3390/w14213423.

Al-Kahtany, Kh., El-Sorogy, A.S., 2022. Heavy metal contamination of surface seawaters in Abu Ali Island, Saudi Arabia. Arab. J. Geosci. 15, 1662. https://doi.org/10.1007/s12517-022-10949-y.

Al-Kahtany, Kh., El-Sorogy, A.S., 2023. Contamination and health risk assessment of surface sediments along Ras Abu Ali Island, Saudi Arabia. Journal of King Saud University – Science 35, 102509. https://doi.org/10.1016/j.jksus.2022.102509.

Al-Kahtany, Kh., Youssef, M., El-Sorogy, A., 2015. Geochemical and foraminiferal analyses of the bottom sediments of Dammam coast, Arabian gulf, Saudi Arabia. Arab. J. Geosci. 8, 11121–11133. https://doi.org/10.1007/s12517-015-2000-7.

Al-Kahtany, Kh., Nour, H.E., Giacobbe, S., Alharbi, T., El-Sorogy, A.S., 2023. Heavy metal pollution in surface sediments and human health assessment in southern Al-Khobar coast, Saudi Arabia. Mar. Pollut. Bull. 187, 114508. https://doi.org/10.1016/j.marpolbul.2022.114508.

Alshehri, F., Almadani, S., El-Sorogy, A.S., Alwaqdani, E., Alfaifi, H.J., Alharbi, T., 2021. Influence of seawater intrusion and heavy metals contamination on groundwater quality, Red Sea coast, Saudi Arabia. Mar. Pollut. Bull. 165, 112094. https://doi.org/10.1016/j.marpolbul.2021.112094.

Alzahrani, H., El-Sorogy, A.S., Qaysi, S., Alshehri, F., 2023. Contamination and risk assessment of potentially toxic elements in coastal sediments of the area between Al-Jubail and Al-Khafji, Arabian gulf, Saudi Arabia. Water 15, 573. https://doi.org/10.3390/w15030573.

Bello, S., Nasiru, R., Garbab, N.N., Adeyemo, D.J., 2019. Carcinogenic and non-carcinogenic health risk assessment of heavy metals exposure from Shanono and Bagwai artisanal gold mines, Kano state, Nigeria. Scientific African 6, e00197. https://doi.org/10.1016/j.sciaf.2019.e00197.

Bryanin, S.V., Sorokina, O.A., 2019. Effect of soil properties and environmental factors on chemical compositions of forest soils in the Russian Far East. J. Soils Sediments 19, 1130–1138. https://doi.org/10.1007/s11368-018-2141-x.

Chonokhuu, S., Batbold, C., Chuluunpurev, B., Battsengel, E., Dorjsuren, B., Byambaa, B., 2019. Contamination and health risk assessment of heavy metals in the soil of major cities in Mongolia. Int. J. Environ. Res. Public Health 16, 2552. https://doi.org/10.3390/ijerph16142552.

Christodoulou, E.A., Samanidou, V.F., 2007. Multiresidue HPLC analysis of ten quinolones in milk after solid phase extraction: validation according to the European Union decision 2002/657/EC. J. Sep. Sci. 30, 2421–2429.

Demircan, H., El-Sorogy, A.S., Alharbi, T., 2021. Bioerosional structures from the late Pleistocene coral reef, Red Sea coast, Northwest Saudi Arabia. Turk. J. Earth Sci. 30, 22–37. https://doi.org/10.3906/yer-2005-7.

Dissanayake, C.B., Chandrajith, R., 2009. Introduction to Medical Geology, Focus on Tropical Environments. Springer-Verlag, Berlin Heidelberg, p. 297.

El-Sorogy, A.S., 2015. Taphonomic processes of some intertidal gastropod and bivalve shells from northern Red Sea coast. Egypt. Pakistan J. Zool. 47 (5), 1287–1296.

El-Sorogy, A.S., Youssef, M., 2015. Assessment of heavy metal contamination in intertidal gastropod and bivalve shells from central Arabian gulf coastline, Saudi Arabia. J. Afr. Earth Sci. 111, 41–53. https://doi.org/10.1016/j.jafrearsci.2015.07.012.

El-Sorogy, A.S., Tawfik, M., Almadani, S.A., Attiah, A., 2016. Assessment of toxic metals in coastal sediments of the Rosetta area, Mediterranean Sea. Egypt. Environ. Earth Sci. 75, 398. https://doi.org/10.1007/s12665-015-4985-3.

El-Sorogy, A.S., Alharbi, T., Richiano, S., 2018. Bioerosion structures in high-salinity marine environments: a case study from the Al–Khafji coastline. Saudi Arabia. Estuar. Coastal Shelf Sci. 204, 264–272. https://doi.org/10.1016/j.ecss.2018.03.005.

El-Sorogy, A.S., Demircan, H., Alharbi, T., 2020a. *Gastrochaenolites* ichnofacies from intertidal seashells, Al-Khobar coastline, Saudi Arabia. J. Afr. Earth Sci. 171. http://www.ncbi.nlm.nih.gov/pubmed/103943.

El-Sorogy, A.S., Youssef, M., Al-Kahtany, Kh., Saleh, M.M., 2020b. Distribution, source, contamination, and ecological risk status of heavy metals in the Red Sea-Gulf of Aqaba coastal sediments, Saudi Arabia. Mar. Pollut. Bull. 158, 111411. https://doi.org/10.1016/j.marpolbul.2020.111411.

El-Sorogy, A.S., Demircan, H., Al-Kahtany, Kh., 2021. Taphonomic signatures on modern molluscs and corals from Red Sea coast, southern Saudi Arabia. Palaeoworld. https://doi.org/10.1016/j.palwor.2021.07.001.

Goyer, R., 1993. Casarett and Doull's toxicology. Basic Sci. Poisons 19, 623.

Häder, D.P., Helbling, E.W., Villafañe, V.E., 2021. Anthropogenic Pollution of Aquatic Ecosystems. Springer Nature Switzerland, p. 426. https://doi.org/10.1007/978-3-030-75602-4.

Hakanson, L., 1980. An ecological risk index for aquatic pollution control. A sedimentological approach. Water Res. 14, 975–1001. https://doi.org/10.1016/0043-1354(80)90143-8.

Huang, C.C., Cai, L.M., Xu, Y.H., Jie, L., Chen, L.G., Hu, G.C., Jiang, H.H., Xu, X.B., Mei, J.X., 2022. A comprehensive exploration on the health risk quantification assessment of soil potentially toxic elements from different sources around large-scale smelting area. Environ. Monit. Assess. 194 (3), 206. https://doi.org/10.1007/s10661-022-09804-0.

Huang, C.C., Cai, L.M., Xu, Y.H., Jie, L., Hu, G.C., Chen, L.G., Wang, H.Z., Xu, X.B., Mei, J.X., 2023. A comprehensive approach to quantify the source identification and human health risk assessment of toxic elements in park dust. Environ. Geochem. Health 45, 5813–5827. https://doi.org/10.1007/s10653-023-01588-7.

Huy, T.B., Tuyet-Hanh, T.T., Johnston, R., Nguyen-Viet, H., 2014. Assessing health risk due to exposure to arsenic in drinking water in Hanam Province, Vietnam. Int. J. Environ. Res. Public Health 11 (8), 7575–7591.

IARC, 2012. A review of human carcinogens: personal habits and indoor combustions, 100. World Health Organization, Lyon, France.

IRIS, 2020. Program Database. Available online: https://cfpub.epa.gov/ncea/iris/search/index.cfm. accessed on 18 September 2020.

Järup, L., 2003. Hazards of heavy metal contamination. Br. Med. Bull. 68 (1), 167–182. https://doi.org/10.1093/bmb/ldg032.

Kahal, A., El-Sorogy, A.S., Qaysi, S., Almadani, S., Kassem, O.M., Al-Dossari, A., 2020. Contamination and ecological risk assessment of the Red Sea coastal sediments, Southwest Saudi Arabia. Mar. Pollut. Bull. 154, 111125. https://doi.org/10.1016/j.marpolbul.2020.111125.

Kahal, A.Y., El-Sorogy, A.S., Alfaifi, H.J., Almadani, S., Ghrefat, H.A., 2018. Spatial distribution and ecological risk assessment of the coastal surface sediments from the Red Sea, Northwest Saudi Arabia. Mar. Pollut. Bull. 137, 198–208. https://doi.org/10.1016/j.marpolbul.2018.09.053.

Kowalska, J.B., Mazurek, R., Gasiorek, M., Zaleski, T., 2018. Pollution indices as useful tools for the comprehensive evaluation of the degree of soil contamination–a review. Environ. Geochem. Health 40, 2395–2420. https://doi.org/10.1007/s10653-018-0106-z.

Luo, X.S., Ding, J., Xu, B., Wang, Y.J., Li, H.B., Yu, S., 2012. Incorporating bioaccessibility into human health risk assessments of heavy metals in urban park soils. Sci. Total Environ. 424, 88–96. https://doi.org/10.1016/j.scitotenv.2012.02.053.

Ma, J., Pan, L.B., Wang, Q., Lin, C.Y., Duan, X.L., Hou, H., 2016. Estimation of the daily soil/dust (SD) ingestion rate of children from Gansu Province, China via hand-to-mouth contact using tracer elements. Environ. Geochem. Health 40 (1), 295–301. https://doi.org/10.1007/s10653-016-9906-1.

Mao, C., Song, Y., Chen, L., Ji, J., Li, J., Yuan, X., Yang, Z., Ayoko, G.A., Frost, R.L., Theiss, F., 2019. Human health risks of heavy metals in paddy rice based on transfer characteristics of heavy metals from soil to rice. Catena 175, 339–348. https://doi.org/10.1016/j.catena.2018.12.029.

Mondal, P., Lofrano, G., Carotenuto, M., Guida, M., Trifuoggi, M., Libralato, G., Sarkar, S. K., 2021. Health risk and geochemical assessment of trace elements in surface sediment along the Hooghly (Ganges) river estuary (India). Water 13, 110. https://doi.org/10.3390/w13020110.

Naveedullah, Hashmi, M.Z., Yu, C., Shen, H., Duan, D., Shen, C., Lou, L., Chen, Y., 2014. Concentrations and human health risk assessment of selected heavy metals in surface water of the Siling reservoir watershed in Zhejiang Province, China. Pol. J. Environ. Stud. 23 (3), 801–811.

Nishijo, M., Nakagawa, H., Suwazono, Y., Nogawa, K., Kido, T., 2017. Causes of death in patients with Itai-itai disease suffering from severe chronic cadmium poisoning: a nested case-control analysis of a follow-up study in Japan. BMJ Open 7 (7), e015694. https://doi.org/10.1136/bmjopen-2016-015694.

Pan, L., Wang, Y., Ma, J., Hu, Y., Su, B., Fang, G., Wang, L., Xiang, B., 2018a. A review of heavy metal pollution levels and health risk assessment of urban soils in Chinese cities. Environ. Sci. Pollut. Res. 25, 1055–1069. https://doi.org/10.1007/s11356-017-0513-1.

Pan, L., Wang, Y., Ma, J., Hu, Y., Su, B., Fang, G., Wang, L., Xiang, B., 2018b. A review of heavy metal pollution levels and health risk assessment of urban soils in Chinese cities. Environ. Sci. Pollut. Res. 25, 1055–1069. https://doi.org/10.1007/s11356-017-0513-1.

Papadoyannis, I.N., Samanidou, V.F., 2004. Validation of HPLC instrumentation. J. Liq. Chromatogr. Relat. Technol. 27, 753–783.

Rahman, M.S., Kumar, P., Ullah, M., Jolly, Y.N., Akhter, S., Kabir, J., Begum, B.A., Salam, A., 2021. Elemental analysis in surface soil and dust of roadside academic institutions in Dhaka city, Bangladesh and their impact on human health. Environ. Chem. Ecotoxicol. 3, 197–208. https://doi.org/10.1016/j.enceco.2021.06.001.

Rehman, W., Zeb, A., Noor, N., Nawaz, M., 2008. Heavy metal pollution assessment in various industries of Pakistan. Environ. Geol. 55 (2), 353–358. https://doi.org/10.1007/s00254-007-0980-7.

Škrbić, B.D., Marinković, V., 2019. Occurrence, seasonal variety of organochlorine compounds in street dust of Novi Sad, Serbia, and its implication for risk assessment. Sci. Total Environ. 662, 895–902.

Škrbić, B.D., Marinković, V., Antić, I., Gegić, A.P., 2017. Seasonal variation and health risk assessment of organochlorine compounds in urban soils of Novi Sad, Serbia. Chemosphere 181, 101–110.

Škrbić, B.D., Buljovčić, M., Jovanović, G., Antić, I., 2018a. Seasonal, spatial variations and risk assessment of heavy elements in street dust from Novi Sad, Serbia. Chemosphere 2018 (205), 452–462.

Škrbić, B.D., Kadokami, K., Antić, I., 2018b. Survey on the micro-pollutants presence in surface water system of northern Serbia and environmental and health risk assessment. Environ. Res. 166, 130–140.

Škrbić, B.D., Buljovčić, M., Antić, I., 2022. Comprehensive assessment of heavy elements and evaluation of potential human health risk in the urban environment: a case study from Novi Sad, Serbia. Environ. Sci. Pollut. Res. 29, 38551–38566. https://doi.org/10.1007/s11356-022-18733-x.

Song, Q., Li, J., 2014. A review on human health consequences of metals exposure to, e-waste in China. Environ. Pollut. 196C, 450–461. https://doi.org/10.1016/j.envpol.2014.11.004.

Tian, S., Wang, S., Bai, X., Zhou, D., Luo, G., Yang, Y., Hu, Z., Li, C., Deng, Y., Lu, Q., 2020. Ecological security and health risk assessment of soil heavy metals on a village-level scale, based on different land use types. Environ. Geochem. Health 42, 3393–3413. https://doi.org/10.1007/s10653-020-00583-6.

Turekian, K.K., Wedepohl, K.H., 1961. Distribution of the elements in some major units of the Earth's crust. Geol. Soc. Am. Bull. 72, 175–192. https://doi.org/10.1130/0016-7606(1961)72[175:DOTEIS]2.0.CO;2.

USEPA, 2001. Risk assessment guidance for superfund. In: Part A, Process for Conducting Probabilistic Risk Assessment, III. US Environmental Protection Agency, Washington, DC, USA.

USEPA, 2002. Supplemental Guidance for Developing Soil Screening Levels for Superfund Sites. U.S. Environmental Protection Agency, Office of Emergency and Remedial Response, Washington.

Yaroshevsky, A.A., 2006. Abundances of chemical elements in the Earth's crust. Geoch. Internat. 44 (1), 48–55. https://doi.org/10.1134/S001670290601006X.

Yuan, G., Dai, S., Yin, Z., Lu, H., Jia, R., Xu, J., Song, X., Li, L., Shu, Y., Zhao, X., 2014. Toxicological assessment of combined lead and cadmium: acute and sub-chronic toxicity study in rats. Food Chem. Toxicol. 65, 260–268. https://doi.org/10.1016/j.fct.2013.12.041.

Zhao, L., Xu, Y., Hou, H., Shangguan, Y., Li, F., 2013. Source identification and health risk assessment of metals in urban soils around the Tanggu chemical industrial district, Tianjin, China. Sci. Total Environ. 468–469C, 654–662. https://doi.org/10.1016/j.scitotenv.2013.08.094.